Towards Automatically Cleaned Parabolic Trough Collectors

Yousef A. Gharbia*, Said Grami**

**Mechanical Engineering Department*
American University of the Middle East, Kuwait 15435
***Mechanical Engineering Department, Dhofar University, Salalah, Oman*

***Abstract*—Dust accumulation on parabolic trough collectors can lead to significant degradation to their performance, especially in the MENA region. Owing to the nature of the trough profile and the presence of the receiving tube inside the trough, automatic cleaning has not been a feasible option. This paper presents a thermal numerical analysis of the proposed new collector. This collector is similar to the conventional trough except that the top and end-sides of the trough are closed with sheets made of borosilicate material. The top sheet is curved out to improve its mechanical strength, to take advantage of the self-cleaning mechanism as a result of rain or moisture, and to facilitate the automatic cleaning process. This paper compares the performance of a conventional trough with the new ACPTC in terms of overall heat loss. The results have shown that the ACPTC has significantly outperformed the conventional trough.**

***Index Terms*—Solar energy, trough collector, dust accumulation**

Nomenclature

TABLE I
NOMENCLATURE

VARIABLES	
A	section of surface area facing upwards (m^2)
A'	section of surface area facing downwards, towards the mirror surface (m^2)
D	Diameter (m)
F	View factor
h	heat transfer coefficient (W/m^2.K)
k_a	thermal conductivity of air (W/m.K)
k_g	thermal conductivity of the glass tube (W/m.K)
k_m	thermal conductivity of the reflective mirrors (W/m.K)
k_p	thermal conductivity of the cover plate (W/m.K)
VARIABLES	
L	length of the receiving tube (m)
N_u	Nusselt Number
Q_1	heat transfer through the gap of the vacuum tube towards the top glass cover (W)
Q_2	heat transfer through the glass tube material towards the top glass cover (W)
Q_3	heat transfer through the trough cavity towards the top glass cover (W)
Q_4	heat transfer through the top glass cover (W)
Q_5	heat transfer between the top glass cover and the ambient air (W)
Q_6	heat transfer through the gap of the vacuum tube towards the mirror surface(W)
Q_7	heat transfer through the glass tube material towards the mirror surface (W)
Q_8	heat transfer through the trough cavity towards the mirror surface (W)
Q_9	heat transfer through the mirror material (W)
Q_{10}	heat transfer between the mirror external surface and the ambient air (W)
Q_{11}	heat transfer through the gap of the vacuum tube towards the sky (W)
Q_{12}	heat transfer through the glass tube material towards the they sky (W)
Q_{13}	heat transfer between the glass tube external surface and the ambient air (W)
Q_{14}	heat transfer through the gap of the glass tube towards the mirror surface (W)
Q_{15}	heat transfer through the glass tube material towards the mirror surface (W)
Q_{16}	heat transfer between the glass tuber external surface and the ambient air (W)
Qcd	heat transfer by conduction (W)
Qcd'	heat transfer by conduction in direction of reflective mirror (W)
Qcv	heat transfer by radiation (W)
Qcv'	heat transfer by radiation in direction of reflective mirror (W)
$Q_{Total.conventional}$	total heat transfer by all modes for the conventional trough (W)
$Q_{Total.ACPTC}$	total heat transfer by all modes for ACPTC (W)
T	temperature (K)
T_a	ambient air temperature (K)
T'_{gi}	the temperature of the internal surface of the glass tube facing the reflective mirror (K)
T'_{go}	the temperature of the external surface of the glass tube facing the reflective mirror (K)
T_{ro}	the temperature of the external surface of the metal tube (K)
t_c	the thickness of the top cover (m)
UL_{ACPTC}	Overall heat loss coefficient for ACPTC (W/m^{2}K)
SYMBOLS	
ε	emissivity
σ	Stefan-Boltzmann constant (W/(m^{2}K^4))
SUBSCRIPTS	
a_i	air in the trough cavity
a_o	ambient outside air
$ci-co$	from the top cover internal surface to the top cover external surface
$co-ao$	from top cover external surface to the ambient air
$co-sky$	from top cover external surface to the sky
$gi-go$	from glass tube internal surface to glass external surface
$go-ai$	from glass tube external surface to the trough cavity
$mo-gr$	from mirror external surface to the ground
mi	reflecting mirror internal surface

SUBSCRIPTS

$mi-mo$	from mirror internal surface to mirror external surface	ro	receiving tube external surface
mo	reflecting mirror external surface	$ro-ci$	from the receiving tube external surface to the cover plate internal surface
$mo-ao$	from mirror external surface to the ambient air	$ro-gi$	from the receiving tube external surface to the glass tube internal surface
		$ro-mi$	from receiving tube to mirror internal surface

I. INTRODUCTION

THE The recent years have seen increasing interest of concentrated solar power (CSP) for electric power generation in many parts of the world and the MENA region is no exception. There are many CSP projects either under-way or in the planning stages in many countries such as Kuwait, Saudi Arabia, UAE, and Oman. The high solar radiation for most of the year in these countries made CSP very attractive option. One of the biggest challenges for such systems, however, is the high frequency of dusty days and sand storms throughout the year in this region. Data collected by Kuwait Meteorological Center over four years (2010-2013) showed that the number of occurrences of suspended dust storms ranged between 70 to 115 days/yr and between 65 to 90 days/yr for rising dust storms. In 2012 there was as many as 15 sand storms in addition to 90 days of each type of the other storms. Dust accumulates on the reflective surfaces of CSP systems adversely affect their performance.

Charabi and Gastli [1], using GIS and satellite data for solar radiation intensity and dust patterns pertaining to Oman, have shown that the areas which are most suitable for solar application are the same areas that have the highest dust concentration levels. Another study conducted by the Masdar Institute in Abu Dhabi has found that in some instances dust accumulation can reduce the reflectance of the solar collectors by up to 35 % per week [2]. A similar study carried out on trough collectors installed in Iran has shown comparable effects of dust accumulation on trough mirrors [3]. Such high figures call for frequent cleaning to maintain the performance of trough collectors at some acceptable level.

The frequency of cleaning can vary from site to site. For instance, it has been reported that the trough collector system installed at Madinate Zaid near Abu Dhabi may require on average two times cleaning per week [4]. This may not seem much, but when you think of an area of 2.5 km^2 filled with hundreds of trough collectors, you will come to realize the enormity of time and financial cost associated with such a process. In addition also to the concern about the consumption of precious fresh water for cleaning, something which is already under strain in the arid regions of MENA.

Although the effect of dust accumulation on PV panels and solar collectors has been studied extensively by many researchers [5-7], little work has been carried out to finding ways to deal with the problem. Adinoyi and Said have shown that the performance of the PV panels installed in the Eastern Provence of Saudi Arabia degraded by 50% of their peak value when the panels were not cleaned for six months. Grag [8] measured reduction of about 60% in the transmittance of the glass cover of a flat solar collector after 30 days of dust accumulation.

To the authors' knowledge, all trough systems used for electrical power generation are of the open trough type where the cavity of the trough is left open to the atmosphere, and hence it is subjected to the ambient conditions such as wind and dust effects. To maintain a steady performance of such systems, continuous cleaning is required to remove the dust accumulated on the reflector mirrors and on the receiving tube. This problem is of greater concern in areas such as MENA due to the high frequency of dusty days and sand storms throughout the year.

Trough systems, due to their curved profile, do not lend themselves to an automatic cleaning process. The new self-cleaning technology based on hydrophobic coating of mirror surfaces [9] may not be very effective in dusty and dry areas such as the Middle East. The success of such techniques relies on the cleaning effect caused by rain or mist droplets as they roll down a tilted collector. To deal with the dust accumulation problem, one company called Glasspoint came up with a unique design whereby the whole trough field is contained inside a “glasshouse” with an automated cleaning machine sweeping the roof [10]. The cost associated with such approach may render the technique less attractive or only feasible for small scale installations.

In this paper, we introduce a new design whereby the parabolic trough is covered from the top and the sides by thin sheets made of borosilicate material. These sheets have transmissivity of around 94%. The top cover is intentionally chosen to be wider than the span of the trough so that when fitted on the trough it bulges out. This will improve the sheets mechanical strength, activates the self-cleaning property, and makes it possible to install an automatic cleaning machine to clean the top cover. The trough utilizes a conventional vacuum tube mounted at the trough focal point. This design is an improved version of the design reported by the authors [11] in which a flat top sheet was used.
Fig. 1 shows a schematic of the proposed ACPTC with an automated cleaning machine. With rails mounted on the ground, one cleaning machine could sweep an entire row of troughs, thus saving costs. The machine could be fitted with an on-board air compressor to supply compressed air to help with the cleaning process. The new trough performance was compared to a conventional trough with the same dimensions. Both troughs had an aperture of 2.10 m, length of 3.2 m, and a focal point at 60 cm.

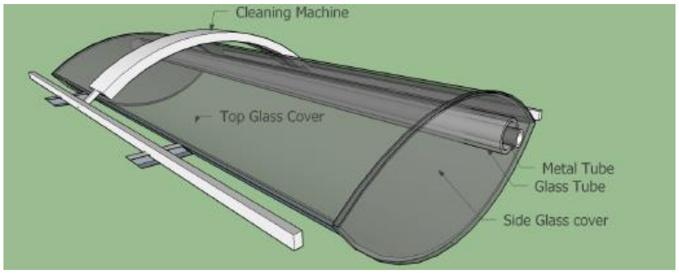

Fig. 1: Schematic of ACPTC

To assess the performance of the new ACPTC, a numerical analysis model has been carried out for both the conventional trough and the ACPTC. Thermal analysis of conventional troughs has been done by many researchers such as Padilla et al. [12], whereby the receiving tube was divided into sections lengthwise to account for heat transfer in the longitudinal direction. The effect of residual pressure inside the vacuum receiving tubes on the receiving tube performance has been studied by Wang et al. [13]. A detailed thermal model of a parabolic trough collector was conducted by Kalogirou [14]. Others have performed numerical models for trough collectors to study the effect of optical errors, tracking error, transmittance and absorptivity of the vacuum receiving tube, heat flux and other factors on trough performance [15-16].

All of the models mentioned above were of the conventional trough type. This paper presents a numerical model for a trough collector closed at the top and the sides by means of borosilicate sheets. It would seem reasonable to hypothesize that since the vacuum tube is isolated from the ambient air and wind, this new trough should result in less heat loss as compared to the conventional one, and consequently should yield superior performance. It is worth mentioning here that the mechanical and thermal stresses analysis of the cover sheet are not within the scope of this paper. Similarly, the discussion will not get into the economical aspect of the new design. In this paper we are merely concerned with the heat loss form the receiving tube assuming isothermal surface temperature of the metal tube. Consequently, control volume analysis of the thermal fluid inside the metal tube is also not within this scope of the work either.

II. HEAT TRANSFER MODEL

The model is written using the Engineering Equation Solver (EES) to take advantage of its capability in determining fluid properties under any given conditions, e.g. temperature and pressure. The trough performance is estimated using the heat energy balance between the external surface of the receiving tube through all the subsequent materials to the ambient air.

Thermal resistance models for both trough collectors with their respective energy models are shown in Fig. 2 and Fig.4. The model assumes uniform surface temperature of the metal receiving tube. This assumption does not introduce much inaccuracy for small collectors [14]. The profile of the trough has also been approximated as a sector of a circle with its circumference made equivalent to the length of the parabolic trough profile. This would maintain the same surface area for the sake of heat transfer calculations by radiation and convection modes. These approximations, although may introduce some inaccuracy, they should not be of much concern, as we are interested in comparing the performance of the two systems rather than the absolute value for each system.

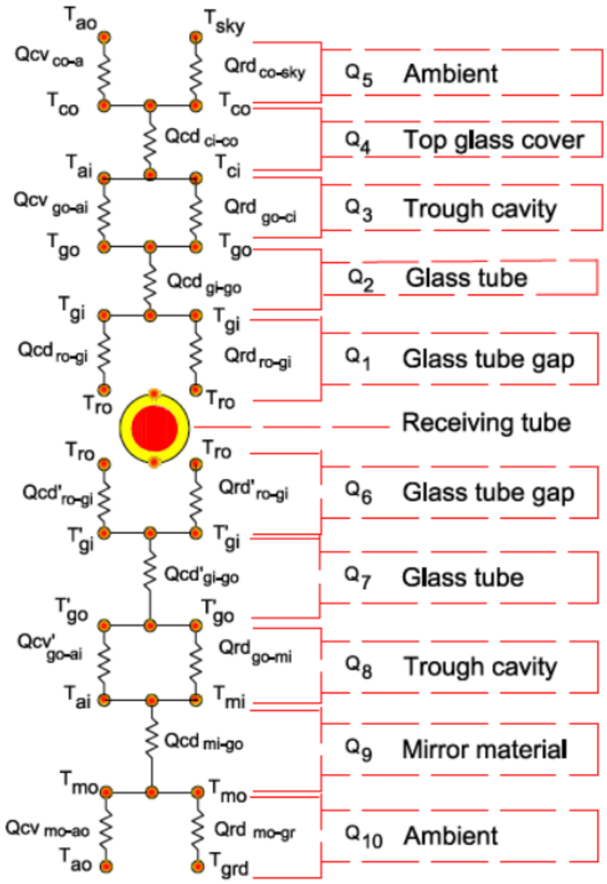

Fig. 2. Heat Transfer model for ACPTC

A. *ACPTC Heat Transfer Model*

The energy model is realized by assuming energy is conserved at each surface of the trough as shown in Fig. 2. The equations were written for heat transfer from the external surface of the receiving metal tube to the ground surface through the reflective mirror in one direction, and between the external surface of the metal tube to the ambient air in the opposite direction.

$$Q_1 = Qrd_{ro-gi} + Qcd_{ro-gi} \tag{1}$$

$$Q_2 = Qcd_{gi-go} \tag{2}$$

$$Q_3 = Qrd_{go-ci} + Qcv_{go-ai} \tag{3}$$

$$Q_4 = Qcd_{ci-co} \tag{4}$$

$$Q_5 = Qrd_{co-sky} + Qcv_{co-ao} \tag{5}$$

Assuming the mirror surface subtends an angle of 160° from the center of the vacuum tube as shown in Fig. 3, breakdown of the above-mentioned equations can be written as shown in Eq. (6) to Eq. (12).

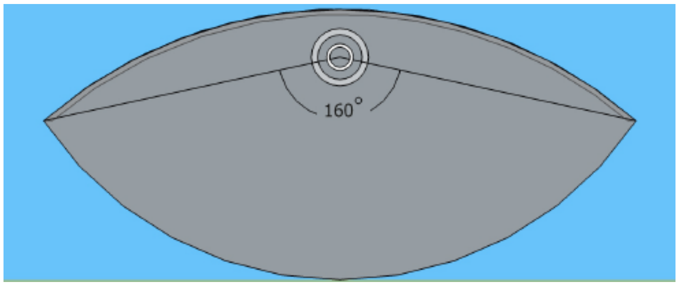

Fig. 3. Side view of the ACPTC

$$Qrd_{ro-gi} = A_{ro}\sigma\left(T_{ro}^{\ 4} - T_{gi}^{\ 4}\right) \cdot \left[\frac{1}{\varepsilon_{ro}} + \frac{1}{F_{ro-gi}} + \left(\frac{1-\varepsilon_{gi}}{\varepsilon_{gi}}\right)\frac{A_{go}}{A_{gi}}\right]^{-1} \tag{6}$$

Where $F_{ro\text{-}gi}$ is the view factor between the metal receiving tube and the internal surface of the glass tube for the section of the tubes facing the trough cover. Since the vacuum tube is assumed under absolute vacuum pressure, The heat transfer by conduction, $Qcd_{ro\text{-}gi}$, is in this case as equal to zero.

$$Qcd_{gi-go} = 2\pi\, k_g\, L\left(T_{gi} - T_{go}\right)\ln\left(\frac{A_{go}}{A_{ci}}\right)^{-1} \tag{7}$$

$$Qrd_{go-ci} = A_{go}\sigma\left(T_{go}^{\ 4} - T_{ci}^{\ 4}\right) \cdot \left[\frac{1}{\varepsilon_{go}} + \frac{1}{F_{go-ci}} + \left(\frac{1-\varepsilon_{ci}}{\varepsilon_{ci}}\right)\frac{A_{go}}{A_{ci}}\right]^{-1} \tag{8}$$

$$Qcv_{go-ai} = A_{go}\, h_{ai}\left(T_{go} - T_{ai}\right) \tag{9}$$

$$Qcd_{ci-co} = A_{ci}\, k_c\left(T_{ci} - T_{co}\right)\Big/ t_c \tag{10}$$

$$Qrd_{co-sky} = \varepsilon_{co}\, A_{co}\sigma\left(T_{co}^4 - T_{sky}^4\right) \tag{11}$$

$$Qcv_{co-ao} = A_{co}\, h_{co}\left(T_{co} - T_{ao}\right) \tag{12}$$

It is to be noted in Eq. 10 above that since the top cover has very shallow curvature, the top cover was treated as a flat plate for simplicity.

Heat flow towards the reflective mirrors, can be estimated using the set of equations listed below. It is to be noted here that since the conditions surrounding the receiving tube are different for the section of the tube facing the top cover and the section facing the reflective mirrors, the variables pertaining to the latter will be denoted with a prime symbol.

$$Q_6 = Qrd'_{ro-gi} + Qcd'_{ro-gi} \tag{13}$$

$$Q_7 = Qcd'_{gi-go} \tag{14}$$

$$Q_8 = Qrd'_{go-mi} + Qcv'_{go-ai} \tag{15}$$

$$Q_9 = Qcd_{mi-mo} \tag{16}$$

$$Q_{10} = Qrd_{mo-gr} + Qcv_{mo-ao} \tag{17}$$

Where;

$$Qrd'_{ro-gi} = A'_{ro}\sigma\left(T_{ro}^{\ 4} - T'^{4}_{gi}\right) \cdot \left[\frac{1}{\varepsilon_{ro}} + \frac{1}{F'_{ro-gi}} + \left(\frac{1-\varepsilon_{gi}}{\varepsilon_{gi}}\right)\frac{A'_{ro}}{A'_{gi}}\right]^{-1} \tag{18}$$

Where A'_{ro} and A'_{gi} are the surface areas of the receiving metal tube and the glass tube facing the reflective mirrors, respectively. $F'_{ro\text{-}gi}$ is the view factor between the receiving metal tube and the glass tube calculated using the crossed-strings method. Again, $Qcd'_{ro\text{-}gi}$ is zero considering absolute vacuum inside the glass tube.

$$Qcd'_{gi-go} = 2\pi\, k_g\, L\left(T'_{gi} - T'_{go}\right) \cdot \left(\ln\frac{A'_{go}}{A'_{gi}}\right)^{-1} \tag{19}$$

$$Qrd'_{go-mi} = A'_{go}\sigma\left(T'^{4}_{go} - T'^{4}_{mi}\right) \cdot \left[\frac{1}{\varepsilon_{go}} + \frac{1}{F_{go-mi}} + \left(\frac{1-\varepsilon_{mi}}{\varepsilon_{mi}}\right)\frac{A'_{go}}{A'_{mi}}\right]^{-1} \tag{20}$$

$$Qcv'_{go-ai} = A'_{go}\, h_{ai}\left(T'_{go} - T'_{ai}\right) \tag{21}$$

$$Qcd_{mi-mo} = 2\pi k_m L\left(T_{mi} - T_{mo}\right)\ln\left(\frac{A_{mo}}{A_{mi}}\right)^{-1} \tag{22}$$

$$Qrd_{mo-gr} = \varepsilon_{mo}\, A_{mo}\sigma\left(T_{mo}^{\ 4} - T_{gr}^4\right) \tag{23}$$

$$Qcv_{mo-ao} = A_{mo}\, h_{mo}\left(T_{mo} - T_{ao}\right) \tag{24}$$

Applying energy balance at the steady state would mean that Q_1, Q_2, Q_3, Q_4, and Q_5 are all equal. Similarly, Q_6, Q_7, $Q8$, Q_9, and Q_{10} are also equal. Using energy balance and a given T_{ro} temperature, all other temperatures can be calculated after going through a number of iterative steps. The ground temperature (T_{gr}) is effectively the ambient air temperature (T_{ao}) ±2°C [17]. Therefore for simplicity, T_{gr} is assumed equivalent to T_{ao} in this model. Once all temperatures were found, the total heat loss from the receiving tube was calculated.

$$Q_{Total-ACPTC} = Q_5 + Q_{10} \tag{25}$$

The overall heat transfer coefficient, UL, which accounts for heat transfer by all modes can then be calculated from the following equation;

$$UL_{ACPTC} = \frac{Q_{Total-ACPTC}}{A_{ro}\left(T_{ro} - T_{ao}\right)} \tag{26}$$

B. Conventional Trough Thermal Model

In a similar manner, the above analysis could be applied to the conventional trough collector. Fig. 4 shows the thermal resistances network through which the heat loss flows from the surface of the receiving tube to the internal surface of the trough mirrors in one direction through the gap of the glass tube and the glass tube material. Heat loss also takes the opposite path to the ambient air.

$$Q_{11} = Qrd_{ro-gi} + Qcd_{ro-gi} \tag{27}$$

$$Q_{12} = Qcd_{gi-go} \tag{28}$$

$$Q_{13} = Qcv_{go-ao} + Qrd_{go-sky} \tag{29}$$

Where;

$$Qrd_{ro-gi} = A_{ro}\sigma\left(T_{ro}^{\ 4} - T_{gi}^{\ 4}\right) \cdot \left[\frac{1}{\varepsilon_{ro}} + \left(\frac{1-\varepsilon_{gi}}{\varepsilon_{gi}}\right)\frac{D_{ro}}{D_{gi}}\right]^{-1} \tag{30}$$

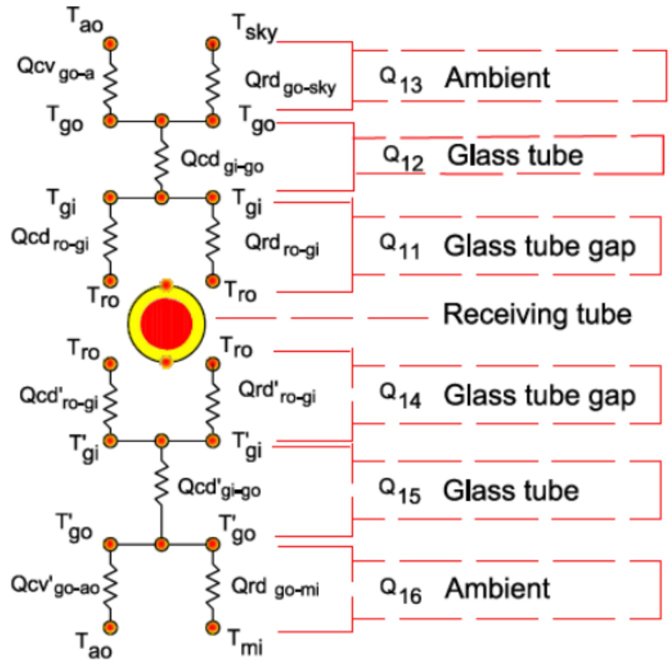

Fig. 4. Heat transfer model for the conventional trough.

$$Qcd_{gi-go} = 2\pi k_g L\left(T_{gi} - T_{go}\right)\ln\left(\frac{A_{go}}{A_{gi}}\right)^{-1} \tag{31}$$

$$Qcv_{go-ao} = A_{go}h_{go}\left(T_{go} - T_{ao}\right) \tag{32}$$

$$Qrd_{go-sky} = \varepsilon_{go}A_{go}\sigma\left(T_{go}^4 - T_{sky}^4\right) \tag{33}$$

There are many expressions that relate the sky temperature (T_{sky}) to other meteorological measured variables. However, in the absence of such measurements, the following simple equation gives reasonable approximation [18].

$$T_{sky} = 0.0553\,T_{ao}^{1.5} \tag{34}$$

Where both T_{sky} and T_{ao} are expressed in degree Kelvin.

The heat loss towards the internal surface of the reflective mirror can be written as:

$$Q_{14} = Qcd'_{ro-gi} + Qrd'_{ro-gi} \tag{35}$$

$$Q_{15} = Qcd'_{gi-go} \tag{36}$$

$$Q_{16} = Qcv'_{go-ao} + Qrd_{go-mi} \tag{37}$$

$$Qrd'_{ro-gi} = A'_{ro}\sigma\left(T_{ro}^{4} - T'^{4}_{gi}\right) \cdot \left[\frac{1}{\varepsilon_{ro}} + \frac{1}{F'_{ro-gi}} + \left(\frac{1-\varepsilon_{gi}}{\varepsilon_{gi}}\right)\frac{A'_{ro}}{A'_{gi}}\right]^{-1} \quad (38)$$

$$Qcd'_{gi-go} = 2\pi L\, k_g \left(T'_{gi} - T'_{go}\right)\left(\ln \frac{A'_{go}}{A'_{gi}}\right)^{-1} \quad (39)$$

$$Qcv'_{go-ao} = A'_{go}\, h_{go}\left(T'_{go} - T'_{ao}\right) \quad (40)$$

$$Qrd'_{go-mi} = A'_{go}\sigma\left(T'^{4}_{go} - T^{4}_{mi}\right) \cdot \left[\frac{1}{\varepsilon_{go}} + \frac{1}{F_{go-mi}} + \left(\frac{1-\varepsilon_{mi}}{\varepsilon_{mi}}\right)\frac{A'_{go}}{A_{mi}}\right]^{-1} \quad (41)$$

Again, for a given T_{ro} and after a number of iterations, the temperatures mentioned above were determined from which the loss in both directions was found. The total heat loss in the case of the conventional trough was estimated by the following.

$$Q_{Total-Covnentional} = Q_{13} + Q_{16} \quad (42)$$

Consequently, the overall heat loss coefficient for the conventional trough can be calculated as follows:

$$UL_{conventional} = \frac{Q_{Total-conventional}}{A_{ro}\left(T_{ro} - T_{ao}\right)} \quad (43)$$

It is worth mentioning here that the heat transfer by conduction mode for Q_1, Q_6, Q_{11}, and Q_{14} are all considered zero since an absolute vacuum is assumed in the vacuum tube annulus. These quantities will remain insignificant for residual pressure, up to 0.013 Pa [19-20].

The convection heat transfer coefficients h_o, h_{mo} and h_{go} in the above equations were calculated using Nusselt Number (Nu) obtained from different empirical formulas reported in [21-22] and elsewhere.

$$h_o = Nu_o\left(\frac{k_{ao}}{L}\right) \quad (44)$$

Where L is the length of the cover plate.

$$Nu_o = 0.3\,\mathrm{Re}^{0.6} \quad for\, 1000 < \mathrm{Re} < 50{,}000 \quad (45)$$

and;

$$h_{mo} = Nu_{mo}\left(\frac{k_{ao}}{D_{mo}}\right) \quad (46)$$

$$Nu_{mo} = 0.26\,\mathrm{Re}^{0.6}\,\mathrm{Pr}^{0.35} \quad for\, 1000 < \mathrm{Re} < 200{,}000 \quad (47)$$

$$h_{go} = Nu_{go}\left(\frac{k_{ao}}{D_{go}}\right) \quad (48)$$

$$Nu_{go} = 0.26\,\mathrm{Re}^{0.6}\,\mathrm{Pr}^{0.35} \quad for\, 1000 < \mathrm{Re} < 200{,}000 \quad (49)$$

All air properties used in these calculations were obtained at the average of ambient air temperature and the temperature of the surface in contact with ambient air.

III. Results and Discussion

Because the two troughs had identical dimensions, made using the same reflective mirrors and subjected to the same ambient conditions, it would be very sensible to base the comparison of the troughs' performance on the heat loss coefficient UL per unit length of the trough.

Fig. 5 shows heat transfer loss coefficient versus the external surface temperature of the metal tube T_{ro}. It can be seen that the ACPTC is experiencing less heat loss as compared to the conventional trough. This reduction could be attributed to the lower average temperature of the surface in contact with the ambient air $(T_{mo}+T_{co})/2$ for ACPTC as compared with the average temperature of the glass tube $(T'_{go}+T_{go})/2$ for the conventional trough, as seen in Fig. 6. For example, for a given receiving tube temperature of T_{ro} = *200° C*, the difference between these two temperatures was found to be around 28° C. This difference continues to grow with the increase of the receiving tube surface temperature. The higher the surface temperature for the conventional trough the higher the heat loss for the conventional trough as compared to the ACPTC. It can be seen from the Fig. 5 that the improvement achieved by ACPTC over the conventional trough is more significant for higher temperature applications with more than 65 % reduction in the overall heat transfer coefficient attained at T_{ro} = 400°C. Since there was no wind blowing inside the closed trough, the heat transfer coefficient, h_i, used for these calculations was that of still air, assumed as 5 W/m^2.K. To examine the sensitivity of variations of h_i on the heat loss, the value of h_i was varied from 3 to 7 W/m^2.K. The results shown in Fig 7 revealed only 8.5 % reduction in *UL* of ACPTC at $T_{ro} = 400\,^{\circ}$C.

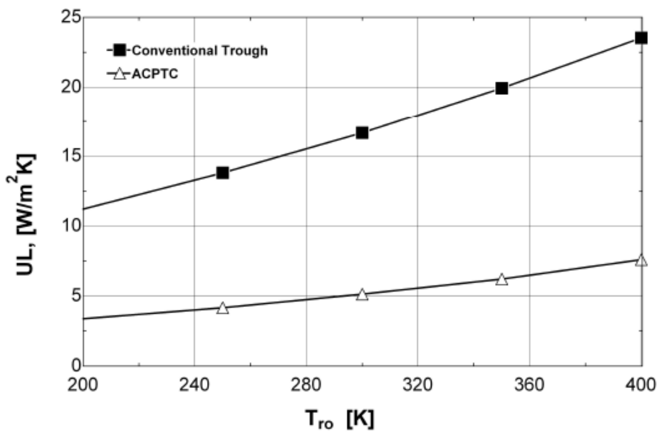

Fig. 5. Heat loss coefficient for ACPTC & the conventional trough

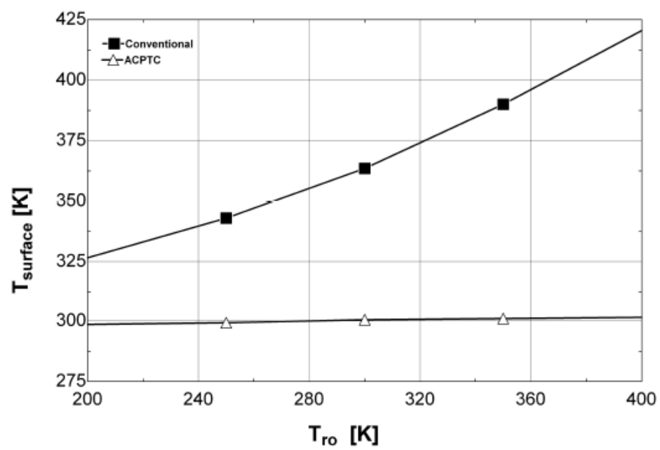

Fig. 6. The temperature of the surface in contact with the ambient air

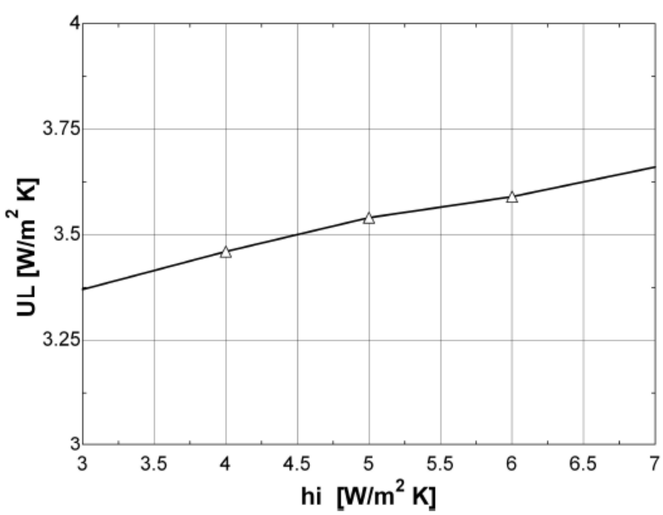

Fig. 7. The effect of the varying the heat transfer coefficient hi inside the ACPTC on the overall heat transfer coefficient

IV. Conclusion

This work shows that the new proposed design should significantly reduce the amount of the heat loss from the receiving tube as compared with the conventional design. This improvement becomes more significant at elevated temperatures. It is worth mentioning here that the cover sheet with transmissivity of 94% would result in less solar radiation reaching the receiving tube as compared with the conventional trough. However since the ACPTA results in about 65% reduction in heat loss, the gains outweigh the losses. Putting the improvement in performance aside, the real advantage of the ACPTC lies in the possibility of adapting an automatic cleaning method. This would mean that the frequency of cleaning parabolic troughs is no longer a problem. With this, troughs can now be cleaned as many times as desired using minimum resources. This would ensure that troughs can steadily maintain their clean-mirror performance, regardless to weather conditions or installation site.

References

[1] Charabi Y., Gastli A.,(2012): Spatio-temporal assessment of dust risk maps for solar energy systems using proxy data, Renewable Energy, 44, 23-31.

[2] Tahboub Z., Dahleh B., and Goebel O., *Solar Mirrors Soiling Campaign Abu Dhabi*, Madar Institute internal report, 2011.

[3] Niknia I., Yaghoubi M., and Hessami R., (2012): A novel experimental method to find dust deposition effect on the performance of parabolic trough solar collectors, International Journal of Environmental Studies, 1-20.

[4] Al-Ali Y. *SHAMS ONE Development Challenges*, Fourth Saudi Solar Energy Forum, May 8-9, 2012.

[5] Adinoyi M., Said S., (2003): Effect of dust accumulation on the power outputs of solar photovoltaic modules, Renewable Energy, 60, 633-636.

[6] Beattie N. S., Moir R. S., Chackoa C., Buffoni G.,Roberts S.H., Pearsall N.M., (2012): Understanding the effects of sand and dust accumulation on photovoltaic modules, Renewable Energy, 48, 448 - 452.

[7] Kaldellis J.K., Kapsali M., (2011): Simulating the dust effect on the energy performance of photovoltaic generators based on experimental measurements, Energy, 36, 5154-5161

[8] Garg HP. (1974): Effect of dirt on transparent covers in flat plate solar energy collectors. Sol Energy, 15, 40, 299-302.

[9] Gaofa H., Chuande Z., Zelun L., (2011): Review of Self-Cleaning Method for Solar Cell Array, Procedia Engineering, 16, 640-645.

[10] Glasspoint (2003): http://www.glasspoint.com/technology/sealed-from-dust/

[11] Gharbia Y. Grami S. Wazwaz A., (2014): Vacuum Cavity Parabolic Trough Collector, 2014 International Mechanical Engineering Congress & Exposition, November 14-20, Montreal, Canada.

[12] Padilla R.V., Demirkaya G., Yogi D., and et al, (2011): Heat transfer analysis of parabolic trough solar receiver, Applied Energy, 88, 5097-5110.

[13] Wang J., Huang X., Gong G., Hao M., Yin F., (2011): A systematic study of the residual gas effect on vacuum solar receiver, Energy Conversion and Management, 52, 2367-2372.

[14] Kalogirou S.A., (2012): A detailed thermal model of a parabolic trough collector receiver, Energy 48, 1, 298-306.

[15] Weidong H., Peng H,, Zeshao C., (2012): Performance simulation of a parabolic trough solar collector, Solar Energy, 86, 746-755

[16] Qibin L., Minlin Y., Jing C., Hongguang J., et al. (2012): Modeling and optimizing parabolic trough solar collector systems using the least squares support vector machine method, Solar Energy, 86, 1973-1980

[17] Gallo, K., Hale R. , Tarpley D., Yunyue Y., (2011): Evaluation of the Relationship between Air and Land Surface Temperature under Clear- and Cloudy-Sky Conditions, J. Appl. Meteor. Climatol, 50, 767-775.

[18] Swinbank W., (1963): Long-wave radiation from clear skies. Quar J R Meteorol Soc; 89(381): 339-48.

[19] Price H., Lu E., Kearney D., Zarza E., Cohen G., Gee R., et al. (2002): Advances in parabolic trough solar power technology, J Sol Energy Eng, 12, 109-17.
[20] Thomas JR., (1979): Heat conduction in partial vacuum. Virginia Polytechnic Institute and State University. Blacksburg, Virginia: U.S. Department of Energy, EM-78-C-04-5367.
[21] Cengel Y., Boles M., (2006): Heat and Mass Transfer: A Practical Approach, Prentice Hall, 3rd Edition, pg 175 and 402.
[22] Duffie J., and Beckman W., (2006): Solar Engineering of Thermal Processes, Wiley, 3rd Edition, pg 166, and 331.

Dr. Yousef Gharbia received his B.S. degree from the Higher Institute of Mechanical and Electric Engineering, Libya, M.S. degree from Univeristi Sains Malaysia, and PhD from the University of New South Wales, Australia, all in Mechanical Engineering in 1992, 1996, and 2004, respectively. Dr. Gharbia has worked as a lecturer and an assistant professor of Mechanical Engineering in many countries like Malaysia, Australia, Oman, and Kuwait. His research interest include renewable energy, water desalination, nano fabrication, and friction models.

Dr. Said Grami received a BS Degree in Electro-mechanical Engineering from ENIM Morocco, a M.S. Degree in automation from Polytechnic College, Montreal, CANADA, and PhD degree in Control Engineering from College of Technology, Quebec University, Montreal, CANADA. He is currently an assistant professor in echatronics department at Dhofar nate of Oman. His research focuses olar energy.